ACTA SCIENTIAE

ISSN: 2178-7727

Stability Of Embankments Over Geogrid-Encased Stone Column-Improved Soft Soils

Mohamed LABED; Naas ALLOUT

Civil Engineering Department, University of Djelfa, Djelfa, Algeria.
Civil Engineering Research Laboratory, University of Biskra, BP 145, 07000 Biskra, Algeria;
E-mail: mohamed.labed@univ-djelfa.dz
Laboratory of Mechanical and Materials Development, Civil Engineering Department, Ziane Achour University of Djelfa.
E-mail: n.allout@univ-djelfa.dz

ABSTRACT

The soft soils pose a problem of the earthwork's stability; the treatment of this type of soil by a group of stone columns is a recent technique which makes it possible to ensure a good resistance of the vertical stresses. This paper focuses on the numerical analysis of embankment over geogrid-encased stone column-improved soft soil. The finite difference code Fast Lagrangian Analysis of Continua in 3 Dimensions (FLAC3D) was used to determine the factor of safety and the horizontal displacements of the stone columns. The embankment fill, the subsoil, and the stone columns were modeled by an elasto-plastic model with a Mohr-Coulomb yield criterion and associated flow rule. In this study, several geometrical and mechanical parameters have been considered, such as the stiffness modulus of the geosynthetic, the embankment fill height, friction angle and stiffness of the stone columns, the undrained cohesion and soft soils depth. The factors of the security obtained by a three-dimensional computation were compared with the results of a two-dimensional computation. The results of this study show the influence of the diameter and the spacing of the stone columns on the factor of safety.

Keywords: Embankment; Factor of Safety; Finite differences method; Geogrid; Soft soils; Stone column.

INTRODUCTION

The slope stability analysis is an important problem for geotechnical engineers. Many methods and techniques have been developed for studying the problem of landslides, by making different assumptions about the shape and location of the sliding surface; nevertheless, some results show a significant dispersion of the factor of safety. The limit equilibrium method (Bishop 1955; Petterson 1955; Fellenius 1936) is commonly used. Finite element or finite difference modeling allows the study of various phenomena affecting slope stability (Dawson et al. 1999; Griffiths et Lane 1999; Lyamin et Sloan 2002; Cheng et al. 2007; Liu et Shao 2015; Tschuchnigg et al. 2015; Luo et al. 2016). These approaches define the factor of safety by simply reducing the strength characteristics until failure occurs (c-φ reduction method). Kupka et al. (2009) conducted a comparative study between the two methods to demonstrate the effect of considering inter-slice forces on the factor of safety.

The stone columns are widely used to solve stability problems in structures built on soft soils. This treatment method involves replacing a portion of the in-situ soil with a granular material that takes a high internal friction angle and negligible cohesion. Hughes and Withers (1974) conducted an extensive series of tests on an isolated ballasted column vertically loaded to failure in normally consolidated clay, which confirmed the increase in bearing capacity. Balaam and Booker (1985) presented a finite element numerical analysis to study the settlement of a rigid foundation placed on a layer of clay treated by stone columns, and they found that this treatment technique reduces soil settlement.
It is possible to study both flexible and rigid foundations under concentrated or uniformly distributed loads on different types of soils treated with stone columns (Madhav and Vitkar 1978; Bouassida et al. 1995; Dhouib and Blondeau 2005; Choobbasti et al. 2011; Gniel and Bouazza 2009; Afshar and Ghazavi 2014; Mohanty and Samanta 2015).

ISSN: 2178-7727

The problem of an embankment over a soft soil reinforced by stone columns has been addressed by several authors. Borges et al. (2009) considered an embankment fill on top of a soft clay layer treated with stone columns, where they studied the influence of spacing, diameter, and deformation modulus of the stone columns, as well as the stiffness of geosynthetic layers. The obtained results allowed them to propose a method for determining stress distribution above the stone columns.

The stability of an embankment on soft soil treated with stone columns has been the subject of numerical and theoretical studies. Rowe and Soderma (1985) used the method of limit equilibrium to study the short-term stability of an embankment fill reinforced by geotextile on a purely cohesive soil. Giannaros and Tsiambaos (1997) presented a parametric study using Dimaggio's approach (1978) to analyze the stability of an embankment on soft soil treated with stone columns.

Abusharar and Han (2011) utilized the FLAC code to examine the stability of an embankment on soft soil treated with stone columns. The factor of safety was determined through two approaches: the first one was based on an individual column model, and the second approach adopted the equivalent homogenized areas method. The comparative study revealed that the factor of safety values obtained through the equivalent homogenized areas method were higher than those from the individual column model.

Deb et al. (2012) employed the genetic algorithm method to locate the critical failure surface and optimize the factor of safety for an embankment reinforced by geosynthetics, constructed on a layer of soft clay treated with stone columns reinforced by geosynthetics. The study demonstrated that a genetic algorithm can be successfully used to locate the critical failure surface in the stone column. In summary, these studies explored different numerical methods, such as the FLAC code and the genetic algorithm, to analyze the stability of an embankment on compressible soil treated with stone columns and geosynthetics. They contributed to enhancing the understanding of the behavior of such reinforced soil structures and the factors influencing their stability.

Zhang et al. (2014) studies the stability of an unreinforced embankment over soft clay treated with stone columns. They compared the factor of safety results obtained through three methods: three-dimensional analysis using the FLAC3D code, the method of equivalent walls, and the equivalent homogenized medium method. Their research showed that all three methods provided factor of safety values in good agreement. Chen et al. (2015) conducted physical model tests and three-dimensional numerical finite element modeling to study the behavior of a uniformly loaded embankment placed on a soft soil treated with geosynthetics encased stone columns. They observed a bending failure of the reinforced columns.

More recently, Mohapatra and Rajagopal (2016) presented a finite difference analysis to study the stability of an embankment constructed on soft clay treated with stone columns encapsulated by geosynthetics. They performed a parametric study on geometric parameters (fill height and spacing of stone columns) and mechanical soil parameters (friction angle of the stone and compressibility of the soft clay). Their findings indicated that this treatment technique enhances the stability of the embankment.

The numerical modeling with the Finite element or finite difference methods for studying soil stability problems has become highly reliable. This technique allows determining the factor of safety using the "c-φ reduction" method. The c-φ reduction method involves reducing the cohesion and internal friction angle of the soil until failure of the mass is numerically represented when it is not possible to find an admissible stress state in equilibrium with the applied loads. The calculation also provides information about the failure mechanism found by the numerical analysis. The cohesion (c) and the internal friction angle of the soil (φ) for each test value of the factor of safety are adjusted according to the following equations:

$$c^{test} = \frac{1}{F_s^{test}} c \qquad (1)$$

ISSN: 2178-7727

$$\varphi^{test} = \arctan\left(\frac{1}{F_s^{test}} \tan\varphi\right) \qquad (2)$$

In this study, the problem of interaction between an embankment and a soft soil improved by encapsulated stone columns with geosynthetics is analyzed using the FLAC3D code (2006). The primary objective of this study is to calculate numerically the factor of safety in order to provide construction recommendations related to the geometry and geomechanically characteristics of the stone columns.

The study also examines different modeling approaches for the stone columns, and the factor of safety results obtained from three-dimensional numerical calculations are compared with those obtained from equivalent wall methods.

EQUIVALENT CHARACTERISTICS OF GEOSYNTHETICS ENCASED STONE COLUMNS

One of the major negatives of treating a soft soil with stone columns is the lack of confinement. Encapsulating the columns with a geosynthetic layer helps to address this weakness, increasing the cohesion and elastic modulus of the composite material. In the literature, many authors have attempted to replace the characteristics of the complex material (stone, geosynthetics) with equivalent characteristics of homogeneous material.

The process of determining equivalent characteristics involves simplifying the behavior of the composite system into an equivalent material that represents its overall response. This approach is used to simplify the numerical analysis and make it computationally more efficient while still capturing the essential behavior of the treated soil.

Apparent cohesion of geosynthetics encased stone column

It is possible to consider the combination of the soil and geosynthetic layers as a homogenous material. Numerous studies have been conducted on the soil/geosynthetic interaction to determine the apparent cohesion of the material to be used (Bathurst and Carpurapu 1993; Reiffsteck 1996; Rajagopal et al. 1998; Malarvizhi and Ilamparuthi 2008).

Bathurst and Carpurapu (1993) proposed a relationship to predict the apparent cohesion of the stone column encapsulated by geosynthetics. This relationship allows researchers and engineers to estimate the apparent cohesion of the composite material, which takes into account the contribution of both the stone and the geosynthetic reinforcement.

$$c_{ce} = \frac{\Delta\sigma_{3g}}{2} \tan\left(\frac{\pi}{4} + \frac{\varphi_c}{2}\right) \qquad (3)$$

Where:

$$\Delta\sigma_{3g} = \frac{2E_g \varepsilon_c}{d\left(1-\varepsilon_a\right)} \qquad (4)$$

$$\varepsilon_c = \frac{\left(1-\sqrt{1-\varepsilon_a}\right)}{1-\varepsilon_a} \qquad (5)$$

In which c_{ce}, $\Delta\sigma_{3g}$,E_g, ε_c, ε_c and d are the apparent cohesion, the increased confining pressure, the modulus of the membrane (kN/m), the circumferential strain, the axial strain and the original diameter of the column, respectively.

Malarvizhi and Ilamparuthi (2008) conducted an extensive series of tests on a physical model and compared it with a numerical model. This study provides the apparent cohesion using the following relationship:

$$c_{ce} = \frac{\Delta\sigma_{1g}}{2} \tan\left(\frac{\pi}{4} - \frac{\varphi_c}{2}\right) + \frac{\Delta\sigma_{3g}}{2} \tan\left(\frac{\pi}{4} + \frac{\varphi_c}{2}\right) \qquad (6)$$

ISSN: 2178-7727

Weher:

$$\Delta\sigma_{1g} = \frac{\pi d E_g \varepsilon_a \left(1-\varepsilon_a\right)}{A_0} \qquad (7)$$

In which $\Delta\sigma_{1g}$, d_ε and A_c are the increased of the axial pressure, the diameter of the column at axial strain ε and the areas of column respectively.

In this study, a three-dimensional numerical modeling of the triaxial test on a stone column with and without encapsulation geosynthetics was conducted to determine the apparent cohesion, as illustrated in Figure 1. The column is a cylinder with a diameter (d_c) of 0.80 m and a height of 1.60 m. The behavior of the stone follows an elastic-perfectly plastic model, and the Mohr-Coulomb criterion with the associated flow rule was adopted. The values of the stone parameters are presented in Table 1. The geosynthetic layer is modeled using the "geogrid" type structural element. The soil-geogrid interface is characterized by cohesion (c_{gs}), friction angle (φ_{gs}), and the stiffness of the spring (k). Sliding occurs within the stone and not at the soil-reinforcement interface ($\varphi_{gs} = \varphi_c$ and $c_{gs} = c_c$). The values of the geogrid element parameters are provided in Table 2. The results obtained from these simulations will contribute to the understanding and optimization of the use of geosynthetics to enhance the performance of stone columns in geotechnical engineering applications.

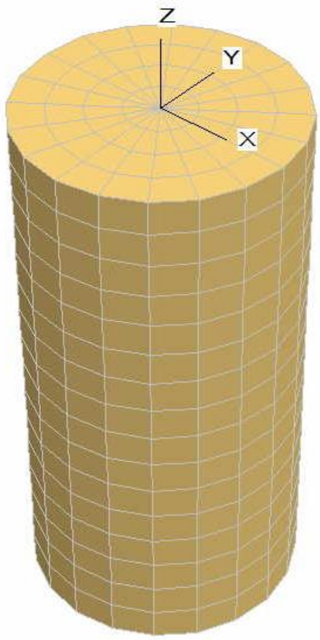

Fig. 1. Compression test model of the stone column.

In the numerical modeling, three different values of isotropic stress (σ_3) were repeated for both cases, with and without encapsulation by geosynthetics. In each case, the Mohr circles were plotted, and the intrinsic strength lines of the stone and the composite material (stone, geosynthetics) were determined, as illustrated in Figure 2.

The apparent cohesion determined using the relationship of Bathurst and Carpurapu (1993) is c_{ce} = 12.6 kPa. Furthermore, using the relationships of Malarvizhi and Ilamparuthi (2008) gives an apparent cohesion of c_{ce} = 23.6 kPa. The three-dimensional modeling of the geosynthetic encased stone column with provides an apparent cohesion of c_{ce} = 22.8 kPa. It is evident that the three-dimensional model in this study produces results in excellent agreement with the results obtained using the relationships of Malarvizhi and Ilamparuthi (2008). On the other hand, there is an underestimation of the apparent cohesion found when using the relationship of Bathurst and Carpurapu (1993). Additionally, it is interesting to note that the intrinsic strength curve of the unreinforced stone provides the same mechanical characteristics as the modeled stone ($\varphi_c = 38°$ and $c_c = 0$ kPa).

ISSN: 2178-7727

After comparing the results obtained using the relationships of Bathurst and Carpurapu (1993) and Malarvizhi and Ilamparuthi (2008) with the results from the present study's model, the method of Malarvizhi and Ilamparuthi (2008) is adopted to determine the apparent cohesion of the geosynthetics encased stone columns.

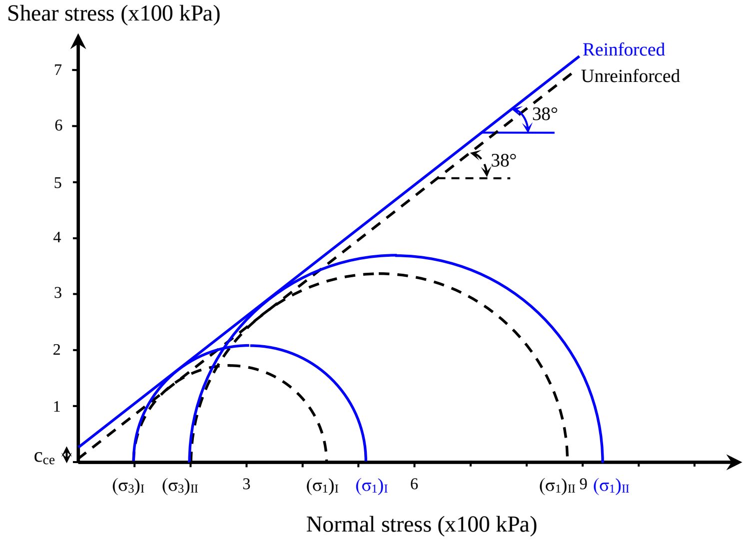

Fig. 2. Mohr circle diagram of unreinforced and reinforced stone columns.

Equivalent Young's modulus and Poisson's ratio of the geosynthetics encased stone Column

A finite element modeling was carried out by Zhou et al. (1998) to study the treatment of soil with geogrid encased stone columns. The study provides the equivalent Young's modulus and Poisson's ratio using the following relationships:

$$E_{ce} = \frac{1+\beta(1-\nu_c)}{1+\beta\left(1-\nu_c-2\nu_c^2\right)} \quad (8)$$

$$\nu_{ce} = \frac{\nu_c}{1+\beta\left(1-\nu_c-2\nu_c^2\right)} \quad (9)$$

Where:

$$\beta = \frac{E_g}{rE_c} \quad (10)$$

In which ν_c, E_c, E_g and r are the Poisson's ratio of the stone, the Young's modulus of the stone, the Young's modulus of the geogrid and the radius of the encased column, respectively.

Indeed, adopting the method proposed by Zhou et al. (1998) to determine the equivalent elastic characteristics of geosynthetics encased stone columns is justified by its ease and simplicity of equivalence.

Equivalent column wall methods

Individual stone columns can be studied as equivalent wall under plane deformation. Numerous methods for equivalencing individual columns have been proposed to replace the columns with equivalent walls. In the present study, we are interested in two equivalence methods: the equivalent shear resistance method and equivalent bending resistance method.

Equivalent shear resistance method:

In this method, the thickness of the equivalent walls and the diameter of different columns are identical (d_w = d_c, where d_w is the thickness of the equivalent wall and d_c is the diameter of the columns), as illustrated in Figure 2 (b). This approach allows for matching the geometry and properties of the columns (Terashi et al. 1991; Cooper and Rose 1999; Tan et al. 2008). In the present study, this method is referred to as ESM (Equivalent shear resistance method).

ISSN: 2178-7727

The parameters of the equivalent walls are estimated using the weighted average parameters of the columns and the soft soil. These parameters are given by the following relationships:

$$A_w.c_w = c_c.A_c + c_s.A_s \quad (11)$$

$$A_w.\tan\varphi_w = A_c.\tan\varphi_c + A_S.\tan\varphi_S \quad (12)$$

$$A_w.\gamma_w = \gamma_c.A_c + \gamma_s.A_s \quad (13)$$

$$A_w.E_w = E_c.A_c + E_s.A_s \quad (14)$$

$$A_w.\nu_w = \nu_c.A_c + \nu_s.A_s \quad (15)$$

In which c_W, φ_W, E_W , ν_W and γ_W are the equivalent cohesion, friction angle, Young's modulus, the Poisson's ratio and unit weight of the equivalent wall, respectively; c_C, φ_C, E_C , ν_C and γ_C are the apparent cohesion, friction angle, Young's modulus, the Poisson's ratio and unit weight of the encased stone column, respectively; c_S, φ_S, E_S , ν_S and γ_S are the cohesion, friction angle, Young's modulus, the Poisson's ratio and unit weight of the soft soil, respectively; A_W, A_C and A_S are the areas of the equivalent wall, the encased stone column and the soft soil, respectively

Equivalent bending resistance method:

Chen et al. (2015) proposed an approach based on the equality of the moment of inertia of the cross-section of the stone column and the moment of inertia of the cross-section of the equivalent wall. The thickness of the equivalent wall is given by the following relationship:

$$\frac{s.d_w^3}{12} = \frac{\pi.d_c^4}{64} \Leftrightarrow d_w = \sqrt[3]{\frac{3.\pi.d_c^4}{16.s}} \quad (16)$$

In the present study, the Equivalent bending resistance method is referred to as EBM. This approach also allows for matching the geometry and properties of the individual stone columns to the equivalent walls. The parameters of the equivalent walls are estimated using the same equivalence relationships as in the ESM method (equations 11-15).

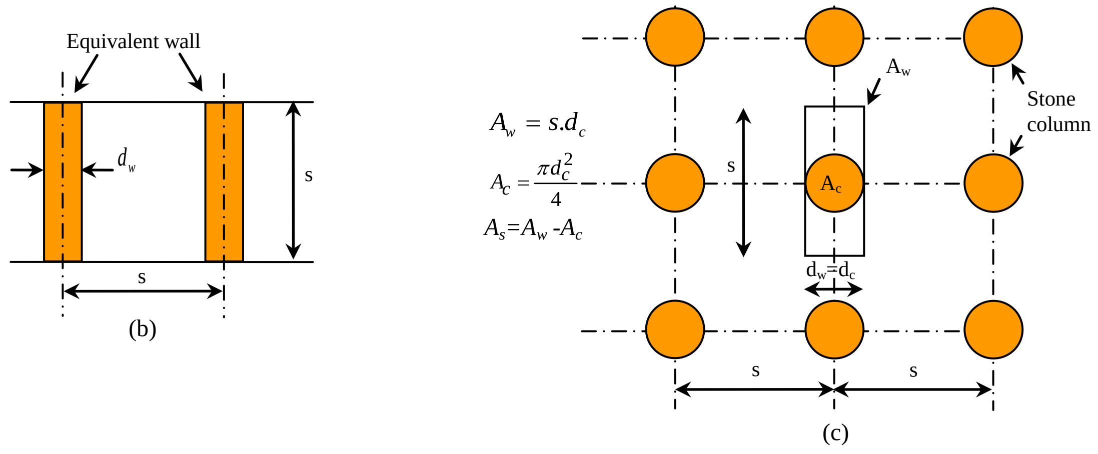

Fig. 3. Two-dimensional equivalency methods: (a) EBM; (b) ESM.

PROBLEM PRESENTATION

The numerical study involves the use of the FLAC3D code (Fast Lagrangian Analysis of Continua in 3 Dimensions) (version 2006) for the analysis of an embankment placed over soft soil treated with geosynthetic-encased stone column. FLAC3D is an explicit finite difference code developed by ITASCA Consulting Group. It is specifically designed for analyzing geotechnical problems involving three-dimensional deformations and behaviors of soil and rock materials.

ACTA SCIENTIAE

ISSN: 2178-7727

In this study, FLAC3D was chosen over FLAC2D to conduct the numerical analysis in three dimensions and to compare the results with those obtained using the two-dimensional model. By using the same code and generic meshing approach, it becomes easier to perform a direct comparison and ensure consistency in the analysis.

The present study focuses on investigating the stability of embankments over geosynthetic-encased stone column-improved soft soils. The study employs the following approaches:

- Equivalent column-wall Methods: Equivalent Shear resistance method (ESM) and Equivalent bending resistance method (EBM) are applied to the study. These methods involve representing the individual stone columns as equivalent walls with specified parameters, facilitating a simplified analysis of the reinforced soil system.
- Three-dimensional numerical analysis of geosynthetic-encased stone column (3D): This approach considers the full three-dimensional deformations and interactions of the materials involved in the system.
- Three-dimensional numerical analysis with equivalent columns (3DCE): Another three-dimensional numerical model is constructed, where the individual stone columns and the geosynthetic are represented as equivalent elements with specific properties. This model allows for a comparative analysis with the 3D model and the equivalent wall methods.

The model presented in Figure 4, originally used by Abusharar and Han (2011), is not specifically intended for examining the stability of the embankment placed on soft soil treated with stone columns encapsulated by geosynthetics. However, in the present study, this model is adopted and modified to serve as the foundational model for investigating the stability of the embankment.

The model represents an embankment with a height of 5 m, inclined at an angle β = 26.6° with respect to the horizontal (a slope of 2H: 1V). To prevent the critical slip surface and facilitate the development of sliding surfaces within the soft soil, a surface layer with a high cohesion value (c) is included. This surface layer ensures that the critical slip surface forms within the treated soft soil rather than at the surface of the embankment.

The embankment and the protective surface are placed on top of a 10 m thick layer of soft soil. This soft soil layer is treated with a network of stone columns that are placed on compacted sand. For the modeling of the two and three-dimensional models, the columns have a circular cross-section with a diameter of $d_c = 0.80$ m. However, to apply the equivalent bending resistance method (EBM), the thickness of the equivalent walls, d_w, is determined using relation (16). On the other hand, for the equivalent shear resistance method (ESM), the thickness of the walls and the diameter of the stone columns are the similar ($d_w = d_c$). Additionally, the spacing s between the columns and equivalent walls in both two-dimensional methods (ESM, EBM) and the three-dimensional models (3D, 3DCE) is set to s = 4 m. Due to the longitudinal and transversal symmetry of the model, only one-quarter of the model is retained, as presented in Figure 4.

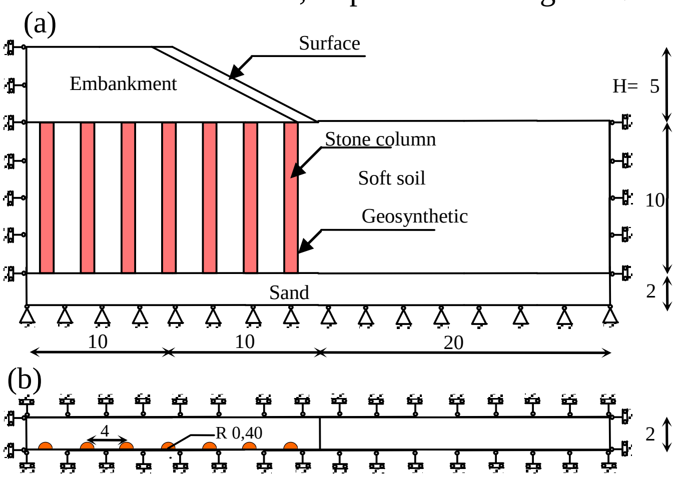

Fig. 4. 3-D finite-element model: (a) cross section; (b) plan view (unit: m).

ISSN: 2178-7727

NUMERICAL MODELING

The numerical modeling involves applying linearly elastic–perfectly plastic materials with Mohr–Coulomb failure criteria to the embankment, surface, soft soil, sand, and stone columns. This criterion is characterized by the following parameters: unit weight (γ), Young's modulus (E), Poisson's ratio (ν), cohesion (c), internal friction angle (φ), and dilatancy angle (ψ) associated with the flow rule (associativity ψ = φ). The values of these parameters used in the analysis are presented in Table 1.

The sand layer beneath the stone columns is assumed to be compacted, resulting in a higher value of Young's modulus (E) to represent a rigid and firm soil.

Table 1: Material properties used in the three and tow dimensional models.

	Diameter or the thickness of wall *d*	Young's modulus *E*	Poisson's ratio *ν*	Unit weight *γ*	Friction angle *φ*	Cohesion *c*
Unit:	m	MPa	-	kg/m^3	°	kPa
Embankment	-	30	0,30	1800	32	0
Surface	-	30	0,30	1800	32	15
Soft soil	-	4	0,45	1600	0	20
Sand	-	100	0,30	1800	30	0
Stone column	0,800	40	0,30	1700	38	0
Equivalent stone column	0,800	50,6	0,07	1700	38	22,8
Equivalent wall (ESM)	0,800	13,1	0,35	1616	7,03	20,4
Equivalent wall (EBM)	0,392	21,5	0,27	1632	14,35	20,9

In the FLAC3D numerical modeling, the geosynthetics are represented using the structural element "geogrid". This requires specifying the mechanical and geometric characteristics of the geosynthetics, such as the stiffness (J), Poisson's ratio (ν), and thickness (t). The shear resistance at the soil-geogrid interface is characterized using a Mohr-Coulomb type friction law. The interface between the soil and geogrid is defined by the cohesion (c_{gs}), the friction angle (φ_{gs}), and the spring stiffness (k). It is important to note that the sliding occurs within the soil and not at the soil-reinforcement interface (φ_{gs} = φc and $c_{gs} = c_c$), indicating that the geogrid is expected to provide reinforcement and not to serve as a sliding surface.

The values of the geogrid parameters are provided in Table 2. The stiffness of the geosynthetic sheet is defined based on the mechanical capabilities of the existing geogrid products available for use in the model. This allows for a realistic representation of the interaction between the geogrid and the soil, enabling accurate simulations of the behavior and response of the reinforced soil system.

Table 2: Properties of the geogrid sheet.

	Stiffness *J*	Poisson's ratio *ν*	Thickness *t*	Friction angle φ_{gs}	Cohesion c_{gs}	Spring stiffness *k*
Unit:	kN/m	-	m	°	kPa	kPa /m
Geogrid	500	0,4	5×10^{-3}	38	0	10^3

Figure 5(a), (b), and (c) display the mesh used for the stability analysis of the embankment fill considering both equivalence methods and the three-dimensional calculation. The mesh contains a large number of elements, which results in a significant computational time.

To account for the boundary conditions, horizontal displacements are constrained at the lateral boundaries, and displacements are fully restrained in all directions at the base of the model. For the two-dimensional calculation, displacement in the third dimension is blocked to treat the problem as a plane strain deformation (Figure 5).

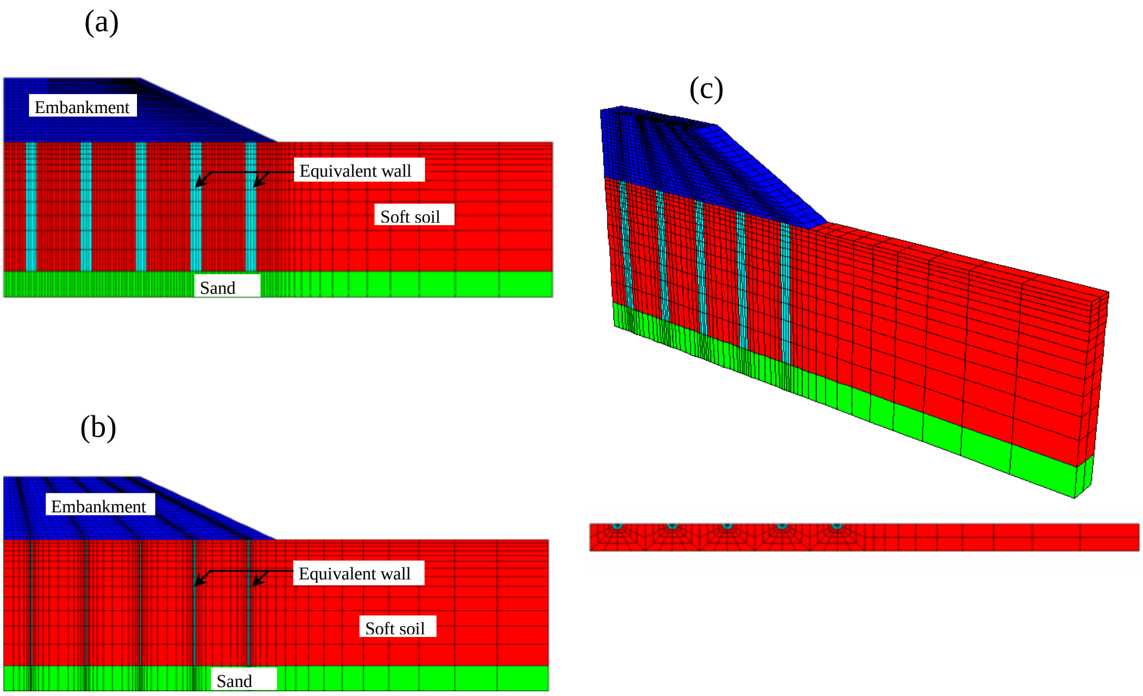

Fig. 5. Finite difference meshes of three and tow dimensional model: (a) ESM; (b) EBM; (c) 3D and 3DCE (3D and top view.).

RESULTS AND DISCUSSIONS

Model validation

The four methods (3D, 3DCE, ESM, EBM) presented above are used to study the stability of an embankment fill placed on soft soil treated with geosynthetics encased stone columns. The factor of safety is determined for both reinforced and unreinforced columns.

For the equivalent bending resistance method (EBM), the equivalent wall thickness (d_w) is set to 0.392 m. This thickness allows determining the areas of the equivalent wall, column, and the soft soil (A_w = 1.568 m^2, A_c = 0.502 m^2, A_s = 1.066 m^2). By using these areas, the characteristics of the equivalent walls are determined using the relationships (11), (12), (13), (14), and (15).

Similarly, the equivalent shear resistance method (ESM), the equivalent wall thickness and the diameter of the different columns are set to be identical, with d_w = 0.80 m. This thickness enables determining the areas of the equivalent wall, column, and the soft soil (A_w = 3.20 m^2, A_c = 0.502 m^2, A_s = 2.70 m^2). The application of relationships (11), (12), (13), (14), and (15) allows determining the characteristics of the equivalent walls for the equivalent shear resistance method (ESM).

Figure 6 shows a comparison of the factors of safety obtained from the present study using the two equivalence methods (ESM, EBM) and the three-dimensional calculations (3D, 3DCE). It is evident that for both unreinforced and reinforced columns, the various approaches introduced in this model yield excellent agreement in the results. Furthermore, both equivalence methods provide more conservative values for the factor of safety.

Additionally, it can be observed that the two-dimensional equivalence methods slightly underestimate the factor of safety when compared to the three-dimensional methods. This difference in results can be attributed to the simplifications inherent in the two-dimensional analysis, which may not fully capture the complexities of the three-dimensional behavior of the reinforced soil system.

ISSN: 2178-7727

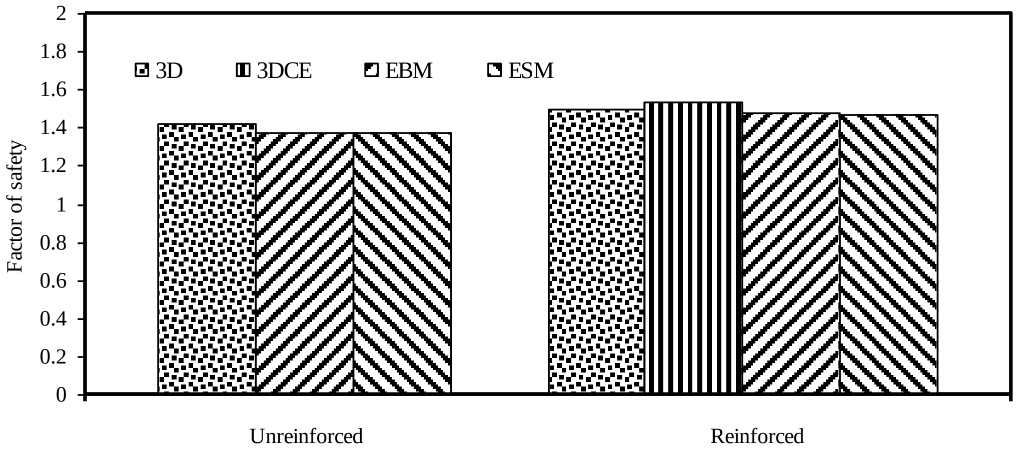

Fig. 6. Factors of safety obtained by different approaches.

Figure 7 shows the shear strain concentration surfaces obtained by the different approaches used in this study (3D, 3DCE, ESM, EBM). It can be observed that there is a discontinuous sliding failure surface obtained by applying the methods of equivalent walls and the three-dimensional models due to the discontinuity in mechanical characteristics between the compressible soil and the stone columns. The use of equivalent wall methods significantly influences the position of the slip surface, allowing the slip surface to develop deeper into the soft soil. Despite this difference in the development of the failure surface, all methods yield factors of safety in excellent agreement, explaining the similarity in the appearance of the shear strain concentration surface.

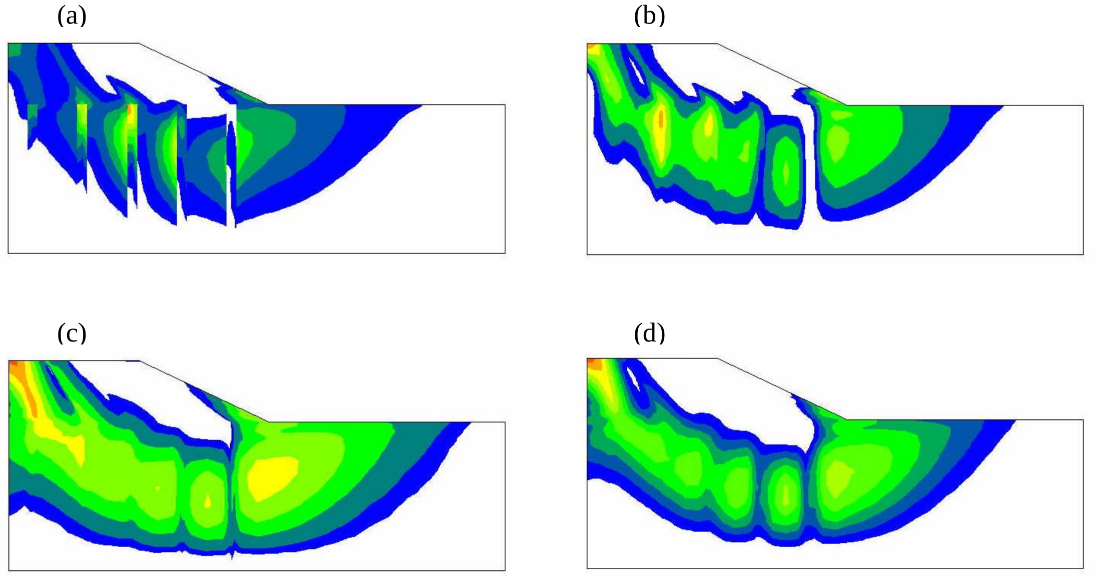

Fig. 7. Contours of maximum shear strain rate obtained by different approaches: (a) 3D; (b) 3DCE; (c) ESM; (d) EBM.

Chen et al. (2015) observed that the horizontal displacements of the columns increase as they move away from the center of the embankment, with the maximum horizontal displacements occurring at the column located under the embankment toe (column #5 in the present study). Figure 8 shows the horizontal displacements at the center of the column under the embankment toe obtained by the present study using the four methods (3D, 3DCE, ESM, EBM). It is evident that the different approaches used in the present models yield significant differences between the results of the three and two-dimensional models. The equivalent wall methods (ESM, EBM) yield a maximum column displacement at a depth of 3 m, while the two three-dimensional methods yield a maximum column displacement at a depth of 1.35 m; Additionally, it is worth noting that the three-dimensional method with equivalent columns slightly overestimates the maximum horizontal displacements compared to the three-dimensional method.

ACTA SCIENTIAE

ISSN: 2178-7727

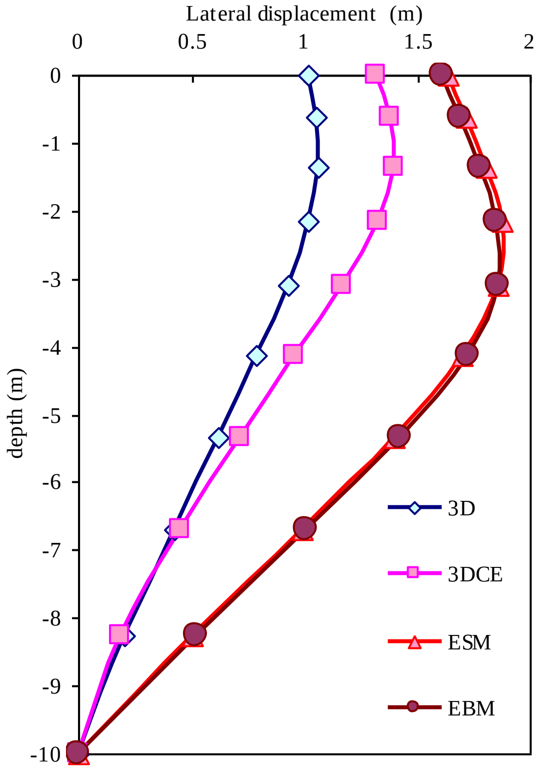

Fig. 8. Lateral displacement of the stone column under the embankment toe obtained by different approaches.

Parametric study

In the present study, after validating the results obtained using different methods, it is observed that the two-dimensional models provide factors of safety and sliding surfaces in excellent agreement when compared to each other, while they overestimate the lateral displacements of the column under the embankment toe compared to the three-dimensional models. On the other hand, there is a negligible difference between the lateral displacements obtained by the three-dimensional model with encapsulated columns and the three-dimensional model with equivalent columns. Therefore, the three-dimensional model with equivalent columns (3DCE) is adopted to examine the factor of safety and lateral displacements of the column under the embankment toe for different spacing-to-diameter (s/d) ratios: s/d = 1.25, 2.5, 5, and 12.5.

Influence of the the embankment height

The factor of safety is directly linked to the embankment height. By varying the embankment fill height in the parametric analysis, the study aims to investigate how this variation impacts the factor of safety and, consequently, its influence on the lateral displacements of the column situated under the embankment toe.

The Figure 9 illustrates the variation of the factor of safety with respect to the height of the embankment (H) for different values of s/d ratio. The height of the embankment is varied between 3 and 7 m with a step of 1 m. The results highlight the significant influence of the embankment height on its stability. As the height of the embankment increases, the applied load on the soft soil also increases, leading to a reduction in the factor of safety.

The spacing, diameter, and encapsulation of the stone columns by geosynthetics play a crucial role in influencing the factor of safety, particularly for embankments with considerable height (greater than 5 meters). For such cases, the increase in embankment height allows the potential sliding surface to develop within the compressible soil and intersect the stone columns. This leads to a decrease in the factor of safety as the column reinforcement is compromised.

ISSN: 2178-7727

On the other hand, for embankments with lower heights, the sliding surface tends to develop within the embankment itself without intersecting the stone columns, resulting in a smaller influence of the s/d ratio on the factor of safety.

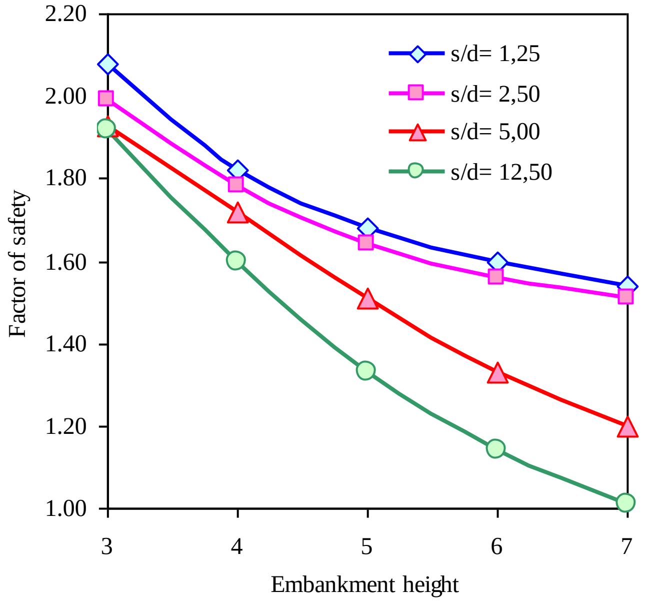

Fig. 9. Influences of embankment fill height.

Figure 10 depicts the horizontal displacements of the center of the column under the embankment toe as a function of depth for different values of the embankment height (H). The results show an increase in the horizontal displacements with the increase in the embankment height. This is due to the fact that as the embankment height increases, the vertical stress above the columns and the soft soil also increase. As a result, the horizontal stress exerted on the stone columns increases, leading to larger horizontal displacements of the column.

Additionally, the increase in the embankment height allows the potential sliding surface to develop at a deeper level within the compressible soil. This explains why the maximum horizontal displacement of the column occurs at a lower depth for higher embankment heights.

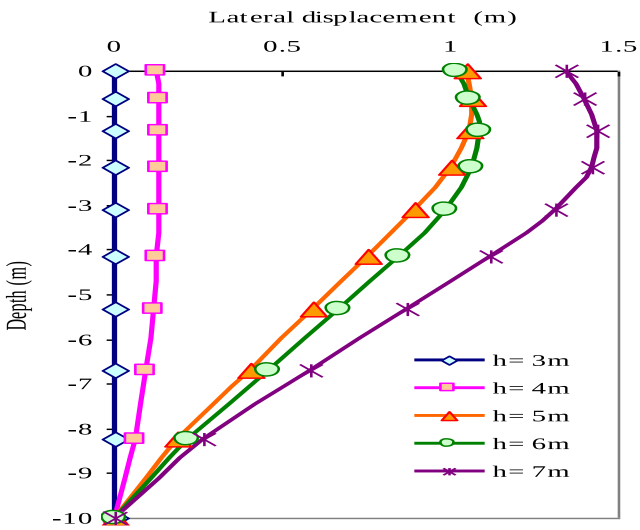

Fig. 10. Lateral displacement of the stone column for different heights of the embankment.

ISSN: 2178-7727

The influence of the stone Young's modulus

The influence of the Young's modulus of the stone on the factor of safety and horizontal displacement of the column under the embankment toe is investigated by performing calculations with Young's modulus of the stone varying between 20 and 400 MPa.

Figure 11 illustrates the variation of the factor of safety with respect to the Young's modulus of the stone for different values of the s/d ratio. From the plot, it can be observed that the influence of the Young's modulus of the stone on the factor of safety remains very slight. This is because the calculation of the factor of safety for slopes is not directly influenced by the Young's modulus of the soils or the stone.

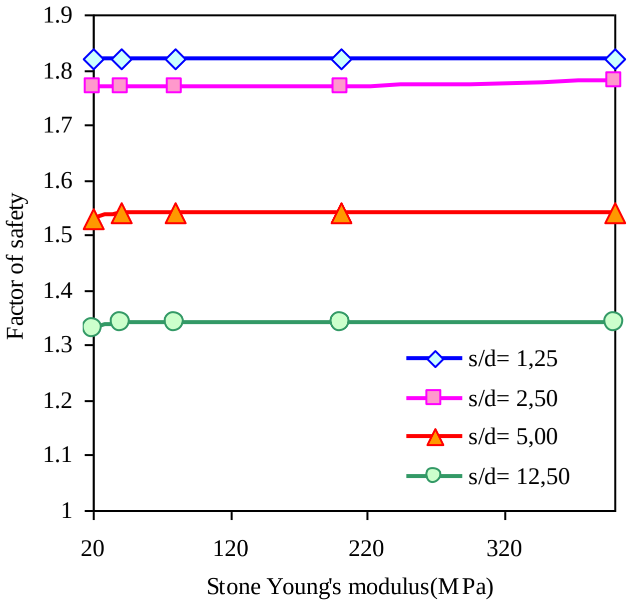

Fig. 11. Influence of Young's modulus of stone column.

Figure 12 shows the variation of the horizontal displacements of the center of the column under the embankment toe as a function of depth for different values of the Young's modulus of the stone. It can be observed that there is a decrease in the horizontal displacements with increasing Young's modulus of the stone. This is because the horizontal displacements of the stone columns are directly influenced by the stiffness or Young's modulus of the stone material.

As the Young's modulus of the stone increases, the stone material becomes stiffer and less prone to deformation under applied loads. This stiffness effectively reduces the lateral movement of the columns and decreases their horizontal displacements.

Influence of the friction angle of the stone:

To study the influence of the friction angle of the stone on the factor of safety and the horizontal displacements of the center of the column under the embankment toe, we perform calculations with a friction angle reaching from 30 to 45 degrees.

Figure 13 illustrates the variation of the factor of safety with respect to the friction angle of the stone columns for different values of the s/d ratio. It is important to note that the impact of the friction angle on the factor of safety remains relatively small for the s/d ratios of 1.25 and 2.50. Similarly, the increase in the factor of safety is particularly modest for the s/d ratios of 5.00 and 12.50.

ISSN: 2178-7727

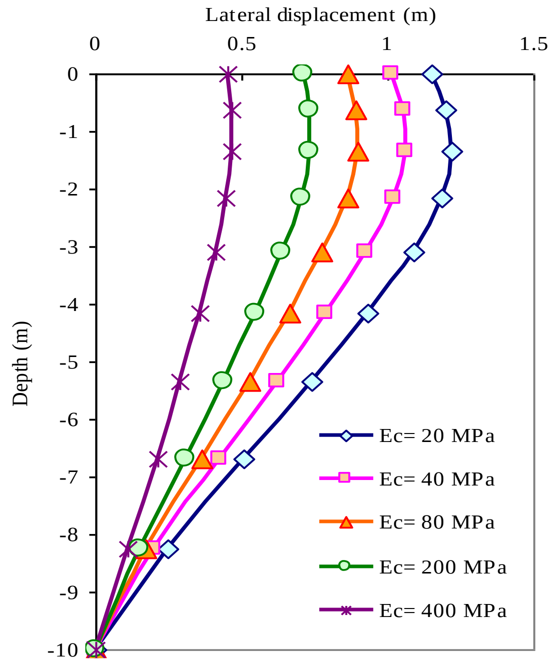

Fig. 12. Lateral displacement of the stone column for different Young's modulus.

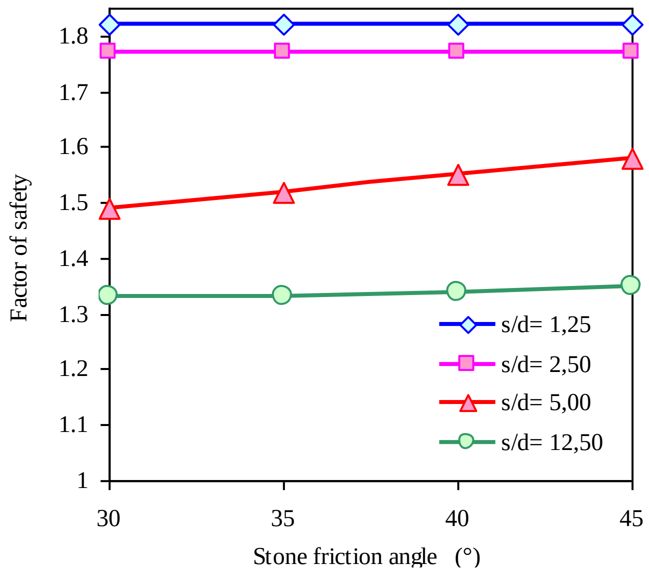

Fig. 13. Influence of friction angle of stone column.

Figure 14 illustrates the variation of the horizontal displacements at the center of the column under the toe of the embankment as a function of depth for different friction angles of the stone. It is evident from the graph that there is a decrease in the horizontal displacements for friction angles of the stone ranging from 30 to 35 degrees. In contrast, there is an increase in the horizontal displacements for friction angles of the stone between 35 and 45 degrees.

The results suggest that within the range of 30 to 35 degrees, increasing the friction angle of the stone leads to improved stability, resulting in reduced horizontal displacements. This can be attributed to the increased mobilization of frictional resistance between the stone and the surrounding soil, which helps to resist lateral movement.

However, beyond a friction angle of 35 degrees, the horizontal displacements start to increase again. This could be due to the formation of a bending failure mechanism in the equivalent columns, which may be less effective in resisting horizontal displacements compared to frictional resistance. Consequently, higher friction angles may lead to a reduction in the overall stability and an increase in horizontal displacements.

ISSN: 2178-7727

The figure also shows that as the friction angle of the stone increases, the depth at which the maximum displacement occurs also rises. This indicates that a higher friction angle allows the sliding surface to floats up in the soft soil, resulting in the maximum displacement point shifting upwards.
Furthermore, for larger friction angles, the rupture of the equivalent columns is likely to occur through a bending failure mechanism, which can be seen as a flexural failure in the graph.

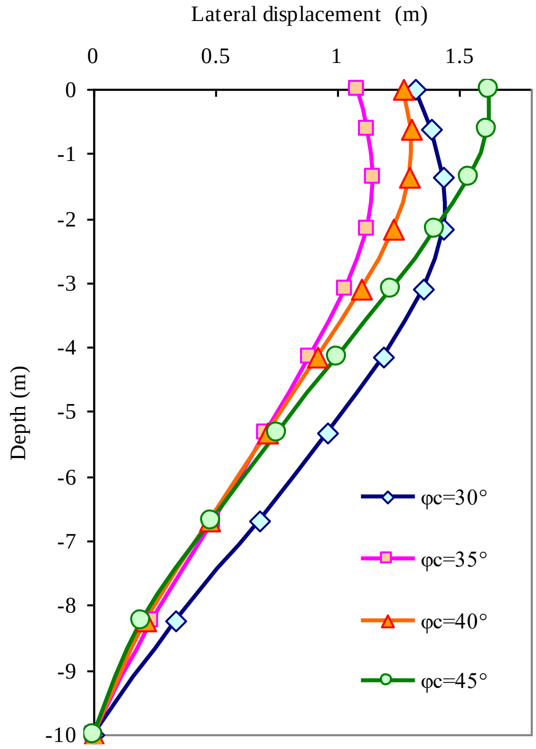

Fig. 14. Lateral displacement of the stone column for different of friction angle of stone column.

Influence of undrained cohesion of the soft Soil

In the case of soft soils, the undrained cohesion is high. It is, therefore, interesting to assess the influence of undrained cohesion on the factor of safety and horizontal displacements at the center of the column under the embankment toe. We conduct calculations with undrained cohesion values reaching from 5 to 20 kPa.
Figure 15 shows the variation of the factor of safety with respect to the undrained cohesion of the soft soil for different values of the s/d ratio. It can be observed that increasing the undrained cohesion improves the capacity of the compressible soil, leading to an increase in the factor of safety. The increase in the factor of safety obtained for s/d ratios of 12.5, 5, 2.5, and 1.25 is approximately 200%, 117%, 47.5%, and 4%, respectively. It is clear that reducing the s/d ratio reduces the rate of increase in the factor of safety when the undrained cohesion is varied from 5 to 20 kPa.

Figure 16 shows the variation of the horizontal displacements at the center of the column under the embankment toe with respect to the depth for different values of the undrained cohesion of the compressible soil. It can be observed that the horizontal displacements decrease with increasing undrained cohesion of the soft soil. This is because the increase in cohesion improves the resistance of the soft soil, resulting in a reduction of the horizontal displacements of the equivalent columns.

ISSN: 2178-7727

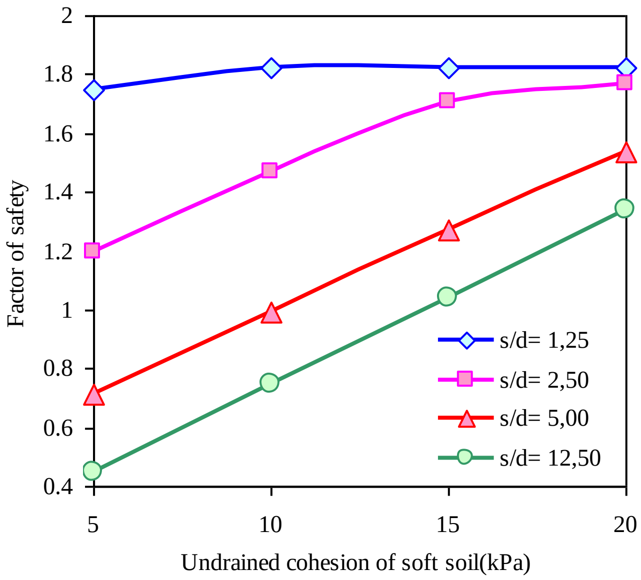

Fig. 15. Influence of undrained cohesion of soft soil.

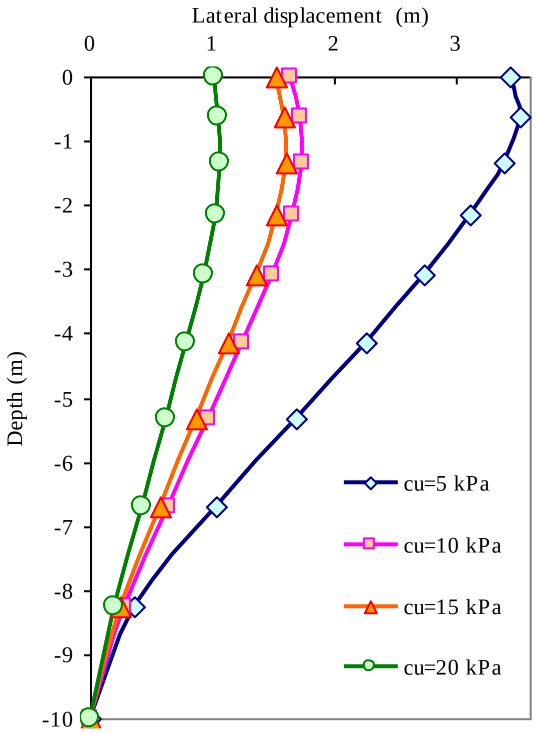

Fig. 16. Lateral displacement of the stone column for different undrained cohesion of soft soil.

Influence of the depth of the soft Soil

The influence of the thickness of the soft soil will be examined in terms of the factor of safety and the horizontal displacements of the column under the embankment toe.

Figure 17 shows the variation of the factor of safety with respect to the depth of the soft soil for different values of the s/d ratio. When the depth of the soft soil increases from 5 m to 35 m, the values of the factor of safety decrease from 1.43 to 1.28 for s/d = 12.50, and from 1.61 to 1.51 for s/d = 5.00. However, for s/d = 2.50, the factor of safety increases from 1.73 to 2.02, and for s/d = 1.25, it increases from 1.75 to 2.95. This result is logical, as a larger depth of the soft soil means a larger volume of soft material for the s/d = 12.50 and 5.00 cases. Conversely, a larger depth of the soft soil means a larger volume of the treatment material for the s/d = 1.25 and 2.50.

ISSN: 2178-7727

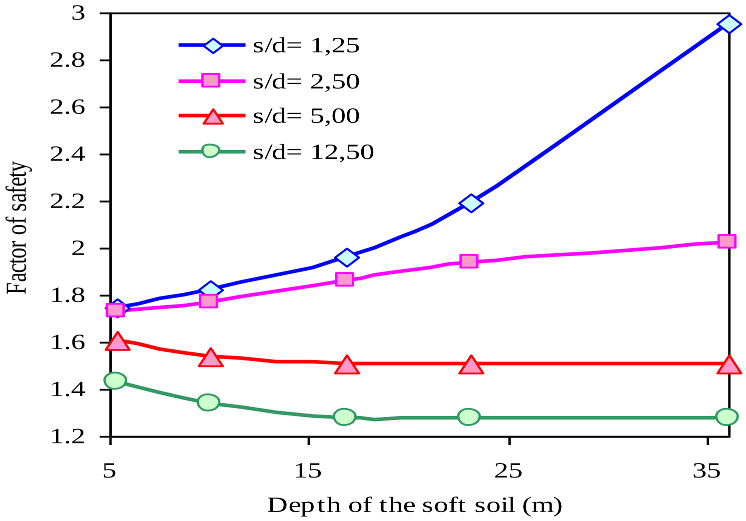

Fig. 17. Influence of the depth of the soft soil.

Figure 18 shows the variation of the horizontal displacements of the column under the embankment toe as a function of the normalized depth for different values of the thickness of the soft soil. It can be observed that the horizontal displacements increase with the increase in the depth of the compressible soil. This is because the increase in depth leads to a reduction in the resistance of the soft soil. As the depth increases, the soft soil has a larger volume, and the load applied to it also increases, resulting in larger horizontal displacements of the equivalent columns.

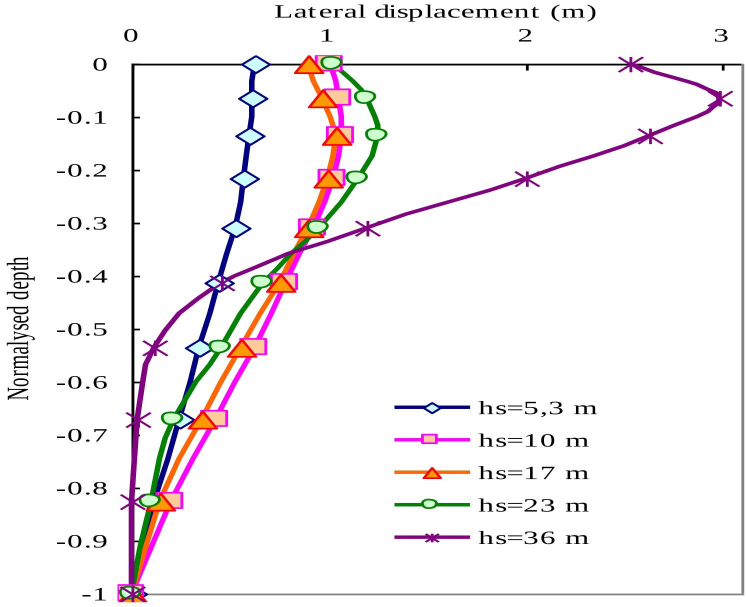

Fig. 18. Lateral displacement of the stone column for different depth of the soft Soil.

The influence of the stiffness of the geosynthetic layer

The stiffness of the geosynthetic layer is directly related to the apparent cohesion and elastic properties of the columns. A higher stiffness of the geosynthetic layer results in less deformation of the columns. For this new series of simulations, the value of the geosynthetic stiffness varies from 0 to 3000 kN/m.

Figure 19 shows the variation of the factor of safety with respect to the stiffness of the geosynthetic layer for different values of the s/d ratio. It is important to note that increasing the stiffness improves the capacity of the stone columns, leading to an increase in the factor of safety. The increase in the factor of safety obtained for s/d ratios of 12.5, 5, 2.5, and 1.25 is 3%, 11%, 1.5%, and 0%, respectively. It can be observed that there is an increasing rate of improvement for s/d ratios between 12.5 and 5. On the other hand, there is a decreasing rate of improvement for s/d ratios between 2.5 and 1.25.

ISSN: 2178-7727

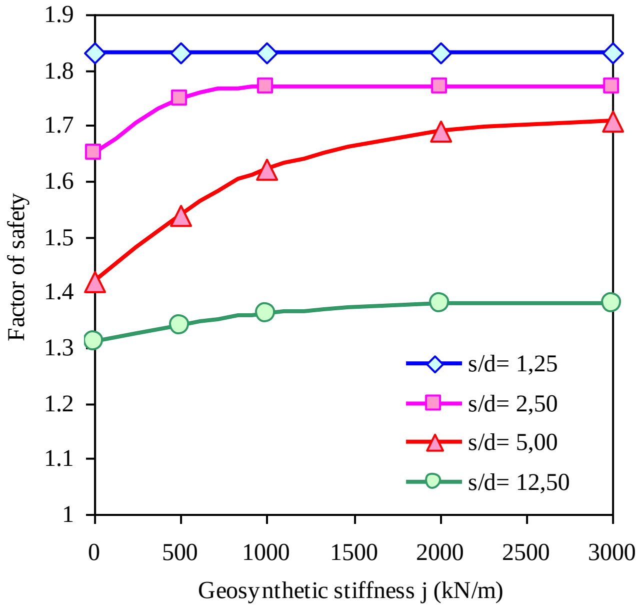

Fig. 19. Influence of the stiffness of the geosynthetic layer.

Figure 20 shows the variation of the horizontal displacements of the column under the embankment toe with respect to the depth for different geosynthetic stiffness values. It is important to note that increasing the geosynthetic stiffness from 0 to 3000 kN/m reduces the horizontal displacements further away from the base of the embankment and increases them closer to the base of the embankment. Figure 20 also shows that increasing the geosynthetic stiffness allows the sliding surface to develop higher in the compressible soil, explaining the emergence of the maximum displacement of the column at a higher depth. This result is in excellent agreement with the findings of Chen et al. (2015), as higher geosynthetic stiffness leads to a bending failure mode of the equivalent columns instead of a shear failure mode.

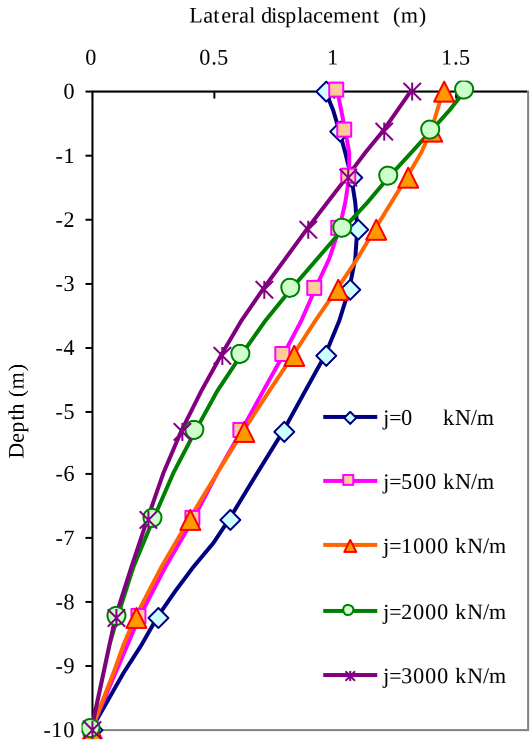

Fig. 20. Lateral displacement of the stone column for different stiffness of the geosynthetic layer.

ISSN: 2178-7727

CONCLUSION

The stability of an embankment built on soft soil treated with geosynthetics encaced stone columns has been examined through two and three-dimensional elastoplastic calculations using FLAC 3D software. In this study, the factor of safety was computed considering different diameters and spacings of the stone columns.
The factors of safety obtained from the two-dimensional equivalence methods show excellent agreement with the three-dimensional calculations for both stone columns with and without reinforcement. Treating the soft soil with encapsulated stone columns using geosynthetics increases the factor of safety.
Increasing the height of the embankment leads to a decrease in the factor of safety and an increase in the horizontal displacements of the stone columns.
Moreover, increasing the Young's modulus and the friction angle of the stone have very little influence on the factor of safety, but they significantly reduce the horizontal displacements of the stone columns.
On the other hand, increasing the undrained cohesion of the compressible soil increases the factor of safety and reduces the horizontal displacements of the stone columns.
It is also important to note that increasing the depth of the soft soil reduces the factor of safety for small spacing ratios and increases it for large spacing ratios. Additionally, increasing the stiffness of the reinforcement geosynthetic significantly increases the factor of safety for moderate spacing-to-diameter ratios, while its influence remains weak for small or large spacing ratios.
Finally, increasing the stiffness of the geosynthetic and the friction angle of the ballast changes the behavior of the stone columns, leading to a binding failure of the equivalent columns instead of a shear failure.

REFERENCES

1. Abusharar, S. W., & Han, J. (2011). Two-dimensional deep-seated slope stability analysis of embankments over stone column-improved soft clay.Engineering Geology, 120(1), 103-110.
2. Afshar, J. N., & Ghazavi, M. (2014). Experimental Studies on Bearing Capacity of Geosynthetic Reinforced Stone Columns. Arabian Journal for Science and Engineering, 39(3), 1559-1571.
3. Balaam, N.P., Booker, J.R., 1985. Effect of stone column yield on settlement of rigid foundation in stabilized clay. International Journal of Numerical and Analytics Methods in Geomechanics 9, 331–351.
4. Bishop A.W. 1955. The use of slip circles in the stability analysis of earth slopes. Géotechnique, 5(1), 7-17
5. Borges, J. L., Domingues, T. S., & Cardoso, A. S. (2009). Embankments on soft soil reinforced with stone columns: numerical analysis and proposal of a new design method. Geotechnical and Geological Engineering, 27(6), 667-679.
6. Bouassida, M., Buhan, P. D., & Dormieux, L. (1995). Bearing capacity of a foundation resting on a soil reinforced by a group of columns. Géotechnique, 45(1), 25-34.
7. Chen, J. F., Li, L. Y., Xue, J. F., & Feng, S. Z. (2015). Failure mechanism of geosynthetic-encased stone columns in soft soils under embankment.Geotextiles and Geomembranes, 43(5), 424-431.
8. Cheng, Y. M., Lansivaara, T., & Wei, W. B. (2007). Two-dimensional slope stability analysis by limit equilibrium and strength reduction methods.Computers and Geotechnics, 34(3), 137-150.
9. Choobbasti, A. J., Zahmatkesh, A., & Noorzad, R. (2011). Performance of stone columns in soft clay: numerical evaluation. Geotechnical and Geological Engineering, 29(5), 675-684.
10. Cooper, M.R., Rose, A.N., 1999. Stone column support for an embankment on deep alluvial soils. Proceedings of the In stitution of Civil Engineers, Geotechnical Engineering 37 (1), 15– 25.
11. Dawson E.M.; Roth W.H., Drescher A. 1999. Slope stability analysis by strength reduction. Géotechnique, 49(6), 835-840
12. Deb, K., Dhar, A., & Bhagat, P. (2012). Evolutionary approach for optimal stability analysis of geosynthetic-reinforced stone column-supported embankments on clay. KSCE Journal of Civil Engineering, 16(7), 1185-1192.
13. Dhouib, A., & Blondeau, F. (2005). Colonnes ballastées : techniques de mise en oeuvre, domaines d'application, comportement, justification, contrôle, axes de recherche et développement. Presses de l'École nationale des ponts et chaussées.
14. DiMaggio, J. A. (1978). Stone columns for highway construction. Technical Report No. FHWA-DP-46-1, US Department of Transport, Federal Highway Administration.
15. Fellenius, W. (1936, July). Calculation of the stability of earth dams. InTransactions of the 2nd congress on large dams, Washington, DC (Vol. 4, pp. 445-463). International Commission on Large Dams (ICOLD) Paris.
16. Giannaros, C., & Tsiambaos, G. (1997). Stabilization of embankment foundations by using stone columns. Geotechnical & Geological Engineering, 15(3), 247-258.

ISSN: 2178-7727

17. Gniel, J., & Bouazza, A. (2009). Improvement of soft soils using geogrid encased stone columns. Geotextiles and Geomembranes, 27(3), 167-175.
18. Griffiths, D. V., & Lane, P. A. (1999). Slope stability analysis by finite elements. Geotechnique, 49(3), 387-403.
19. Hughes JMO, Withers NJ. Reinforcing of soft cohesive soils with stone columns. Ground Eng 1974;7(3):42–9.
20. Karpurapu, R., & Bathurst, R. J. (1993). Large-scale triaxial compression testing of geocell-reinforced granular soils.
21. Liu, S. Y., Shao, L. T., & Li, H. J. (2015). Slope stability analysis using the limit equilibrium method and two finite element methods. Computers and Geotechnics, 63, 291-298.
22. Luo, N., Bathurst, R. J., & Javankhoshdel, S. (2016). Probabilistic stability analysis of simple reinforced slopes by finite element method. Computers and Geotechnics, 77, 45-55.
23. Lyamin, A. V., & Sloan, S. W. (2002). Upper bound limit analysis using linear finite elements and non-linear programming. International Journal for Numerical and Analytical Methods in Geomechanics, 26(2), 181-216.
24. M. Kupka, I. Herle and M. Arnold. Advanced Calculations of Safety Factors for Slope Stability. The 12th International Conference of International Association for Computer Methods and Advances in Geomechanics (IACMAG) 1-6 October, 2008 Goa, India
25. Madhav, M. R., & Vitkar, P. P. (1978). Strip footing on weak clay stabilized with a granular trench or pile. Canadian Geotechnical Journal, 15(4), 605-609.
26. Malarvizhi, S.N., Ilamparuthi, K., 2008. Numerical analysis of encapsulated stone columns. In: The 12th International Conference of International Association for Computer Methods and Advances in Geomechanics (IACMAG), Goa, India, pp. 3719e3726.
27. Mohanty, P., & Samanta, M. (2015). Experimental and Numerical Studies on Response of the Stone Column in Layered Soil. International Journal of Geosynthetics and Ground Engineering, 1(3), 1-14.
28. Mohapatra, S. R., & Rajagopal, K. (2016). Analysis of Failure Mechanism of Geosynthetic-Encased Stone Column Supported Embankments. In Proceeding of the 3rd Pan-American Conference on Geosynthetics, Geo-Americas 2016.
29. Petterson, K.E. 1955. The early history of circular sliding surfaces. Géotechnique, 5: 275–296.
30. Rajagopal K., R.R. Krishnaswamy and Madhavi Latha G. - Behaviour or sand confined with single and multiple
geocells - Geotextiles and geomembranes, n° 17, p 171-184, 1998.
31. Reiffsteck Ph. – Etude du comportement mécanique du géotextile tridimentionnel alvéolaire ARMATER – Analyse numérique et expérimentale - Thèse de doctorat, Université Blaise Pascal Clermont II, 1996.
32. Rowe, R. K., & Soderman, K. L. (1985). An approximate method for estimating the stability of geotextile-reinforced embankments. Canadian Geotechnical Journal, 22(3), 392-398.
33. Tan, S.A., Tjahyono, S., Oo, K.K., 2008. Simplified plane-strain modeling of stone-column reinforced ground. J. Geotech. Geoenviron. 134 (2), 185 -194.
34. Terashi, M., Kitazume, M., Minagawa, S., 1991. Bearing capacity of improved ground by compaction piles. In ASTM Special Technical Publication 1089, Deep Foundation Improvement: Construction and testing, pp. 47–61.
35. Tschuchnigg, F., Schweiger, H. F., Sloan, S. W., Lyamin, A. V., & Raissakis, I. (2015). Comparison of finite element limit analysis and strength reduction techniques. Geotechnique, 65(4), 249-257.
36. Zhang, Z., Han, J., Ye, G., 2014. Numerical investigation on factors for deep-seated slope stability of stone column-supported embankments
37. Zhou, Z.G., Zhang, Q.S., Zheng, J.L., 1998. Analysis of mechanism of improved ground with stone columns reinforced by geogrids. Chin. J. Civ. Eng. 31 (1), 20e25 (in Chinese).